

# Generation of Unstructured Hexahedron-Dominated Conforming Mesh Using Two-Boundary Marching Method

Thomas Wey

*NASA Glenn Research Center, OH 44135*

## **Abstract**

A grid-based all-hexahedron mesh generation method has been modified to create hybrid meshes by merging surface marching grids and inside out grid-based meshes via an advancing front method. It results in a hexahedron-dominated conforming mesh. The surface marching grid is especially suitable for viscous flow calculation.

## **1. Introduction**

The cell-centered based finite volume methods have been widely used in the finite-rate chemistry and particle microphysics flow solvers. It is well known that the most time consuming computation for those flow solvers is resided on the source terms of the species and particle transport equations. A tetrahedral mesh usually increases the element count 4 to 10 fold over a hexahedral mesh for the similar number of vertices in the domain. Thus better efficiency can be achieved by using a hexahedral mesh, since it is directly proportional to the number of elements and the number of species. Also hexahedron provides directional sizing without losing accuracy. For example, a very thin hexahedron close to the surface of a turbine blade performs far better than thin tetrahedron especially if the temperature is the major concerned. The ever-present economic reason to use a hexahedral mesh for the post-combustor trace chemistry simulation and particulate evolution has prompted the effort to develop efficient methods to generate the conforming or overset hexahedral meshes.

Therefore automatically generated all-hexahedron conforming element meshing has become the emerging thrust of mesh generation research [1]. Various techniques have been developed to generate all hexahedral meshes automatically. Most of them are somewhat limited in scope and have different trade-offs. For example, a previous developed all hex generation technique using particle trace analogy [2] will generate extremely excessive dense grid near the seam curves and corners if the preservation of the surface is paramount. It undesirably increases the cost of solving gas and particle emission for jet engines. A new technique has been developed to remove the drawback of the previous method. Instead of all hexahedrons, some other kinds of elements are used to fill the very small portion of the domain. It results in a hexahedron-dominated conforming mesh.

The goal of the present work is to cover the domain by the hexahedrons as much as possible while the pyramids, wedges and tetrahedrons that are treated as degenerate hexahedrons are used to fill the rest of the domain. The current work is built upon an earlier effort involving all hexahedral grid generation [2,3]. Briefly the all hexahedral grid generation starts with a surface bounded algebraic marching grid [4]. The

marching grid is used as the guidance vectors that provide a set of simulated velocity vectors. The particles are released at the fringe points of the background core grid being overset with the marching grid, where the generation of the core grid [3] itself is heavily influenced by the algebraic marching grid. The particle traces under the constraints of the guidance vectors eventually reside on the surface of the algebraic marching grid and form a new set of semi-structured marching grid which starts from the fringe points of the core grid of which the connectivity is in fact a set of quadrilateral shell elements. Thus, a conforming unstructured hexahedral mesh is generated by combining the core grid and particle trace grid.

In the current work, the particle trace grid is allowed to be terminated some layers above of the solid surface. The portion of the original surface bounded marching grid will be kept so that a thin space between the trimmed marching grid and particle trace grid is formed. An advancing front technique [5] is used to fill the space with the pyramids, tetrahedrons and wedges.

## **2. Preprocessing --- Three Major Grids**

To numerically simulate gas and particle emission of jet engines, a unified approach, which is able to generate unstructured (1) overset-hexahedron, (2) all-hexahedron, (3) mostly-hexahedral meshes, is desirable. Three types of component grids are required to be first generated and then proceed to create any one of above mentioned three meshes. These common grids are surface grid, marching grid and core grid.

### **2.1 Surface Grid Generation --Quadrilateral Shell Element**

An angle-based advancing front technique [5] is used to generate surface mesh. The scheme is briefly discussed here for completeness. The union of the curves represents the boundary of the mesh patches (MP). MP is defined as the surface areas to be gridded. For most cases the mesh patches are directly associated with the geometry patches (GP) in the CAD models. The association between the mesh patches and the geometry patches is designed to be one-to-one, one-to-multiple or none for flexibility. The purpose of the one-to-multiple and none associations is to by-pass the extremely small or non-essential geometry patches in the CAD models. Initially the composite boundary curve of a mesh patch is called the front. The front is the union of the frontal elements, which are formed by every three consecutive nodal points. The following steps are involved in the process of generating quadrilateral and triangle mesh.

- Select a frontal element that has the minimum angle in the front.
- If the angle of this frontal element is larger than a prescribed value, for instance 20 degrees is a typical value, then a new point is inserted and one quadrilateral is formed. The location of the new point is influenced by the local size of mesh and subject to internal angle criteria of a quadrilateral.
- If the angle of this frontal element is smaller than the prescribed value then connect two endpoints of the current frontal element to form a triangle and delete the frontal element from the list of the front.
- If the flag of the association between the mesh patches and the geometry patches is turned on, the projection of the new point to geometry patches must be carried out at this moment.

- Update the front.

The mesh generation process terminates when the number of the frontal element is reduced to zero. The types of mesh elements are generally quadrilateral dominated.

## 2.2 Generation of Marching Grid from the Surface Mesh

The surface grid is marched outward into the domain in distinct steps, resulting in layers of semi-structured hexahedrons in the marching direction. For multiply connected body surfaces, one block of marching grid is generated for each block of body or configuration. They will be overset onto each other during the stage of building the composite grids and subject to hole cutting process. There are two important variables for each node in the surface to achieve a successful marching grid, one is the marching step size, the other marching direction. Both variables are relied on a surface characteristics, that is the area change of each node due to virtual offset of surface.

It yields relatively large marching steps in the convex regions where dihedral angle is less than 180 degrees, and small steps in the concave regions where dihedral angle is larger than 180 degrees. The average marching steps are computed by either a constant stretching factor or an exponential function in which marching distance, initial and end spacing in marching direction are required input. For complicated geometry, the marching distances are allowed to be varied from surface mesh patches to surface mesh patches. The initial marching vectors are the normal vectors. However, this may not provide a valid grid since the grid lines may intersect each other in the convex regions. To prevent intersection, the weighted Laplacian type smoothing operation is applied to the components of the marching vectors. The weighting function is once again based on the area change of each node due to virtual offset of surface.

The weighted Laplacian type smoothing operation is applied to grid points to improve the quality of the grids. To control the grid lateral movement, the deviation between two consecutive marching layers for each node should be less than a specified angle. The marching process terminates when the number of steps reach the prescribed value or any of hexahedrons formed between layers of the radiated marching grid has a negative value of volume. One of purposes of generating marching grid is to provide a simulated velocity field to generate particle trace grids later.

## 2.3 Core Grid Generation

A core grid is a grid that encompasses the domain to be gridded. The simplest background core grid is just a cube or brick; however it can be generated by using different schemes. The starting point of the core grid generation is the extraction of the geometric significant points from the radiated marching grid. Suitable clustering and locations of grid points for the core grid can reduce unnecessary refinement in the later stages. The first step of the process is to identify the geometric discontinuities on the first layer of the radiated marching grid that happens to be the surface of the geometry. Any edge of the quadrilateral surface where its dihedral angle is some degrees offset from 180 degrees is identified as a seam segment, the value of 45 degrees is a good number. A point where 3 or more seam segments intersected is called seam corner. A seam curve is made up of a sequence of segments excluding the seam corners. The usage of the seam corners and seam curves are common in the overset grid schemes [6]. The extension of the seam corners and curves from the first layer to the last layer of the marching grid forms the seam columns and seam surfaces. The initial background core

grid needs to be overset with the radiated marching grid. The resolution of the core grid can be increased either by inserting the seam columns and seam surfaces selectively. The quality of the structured grid based core grid may be further improved by relocating the grid points based upon the geometry information conveyed by the radiated marching grid into the core grid. Each grid point of the radiated marching grid will be assigned a scalar that is a function of the rate of area change due to surface virtual offset of the first layer of volume grid. Through tri-linear interpolations, each grid point of the core grid that is contained by the stencil cells of the marching grid will have the variables that indicate a weighting function for grid relocations. The resolution of the core grid can be also be increased by using adaptive mesh refinement strategy described in Reference [7] for 27-node octree based hexahedrons. The major advantages of the structured-grid based core grid over the 27-node octree-based hexahedron are the efficient use of the computer memory and the easiness of relocation scheme.

For rapid-prototype purpose, an overset-hexahedron grid can be very quickly generated by computing the inter-grid interfaces between the marching grid and core grids. It has been reported in detailed in Reference [3]. If the usage of all-hexahedron mesh is preferred, the so-called particle trace grid is needed for this purpose [2]. In this work, the third option is described.

### **3. Two-Boundary Marching Method**

In this abstract, the two-boundary marching method is illustrated through the following examples.

#### **4. Example 1**

A turbine vane based on a film-cooled engine design is used as the geometry. There are twelve slots on the surface. Since the preservation of the geometry is paramount, the grid-based inside out method such as particle trace analogy may not capture the holes exactly. The steps of the current method are:

1. Generates algebraic marching grid from the turbine vane surface which includes blade and cooling holes.
2. Generates passage grid which is heavily influenced by turbine marching grid.
3. Builds particle trace grid guided by turbine marching grid. Let it terminate before reaching turbine vane surface.
4. A thin space is formed between two marching grids shown in Figure 1.
5. Multiple fronts or sub domains between two opposite surfaces are created using shortest distance strategy shown in Figures 2 and 3
6. Volume grid is generated in the thin space using an advancing front method by partitioning the sub domains into pyramids, tetrahedrons and wedges. (see Figures 4, 5 and 6.)

Disparity of grid resolutions of this example is purposely created to show the robust and flexibility of the method.

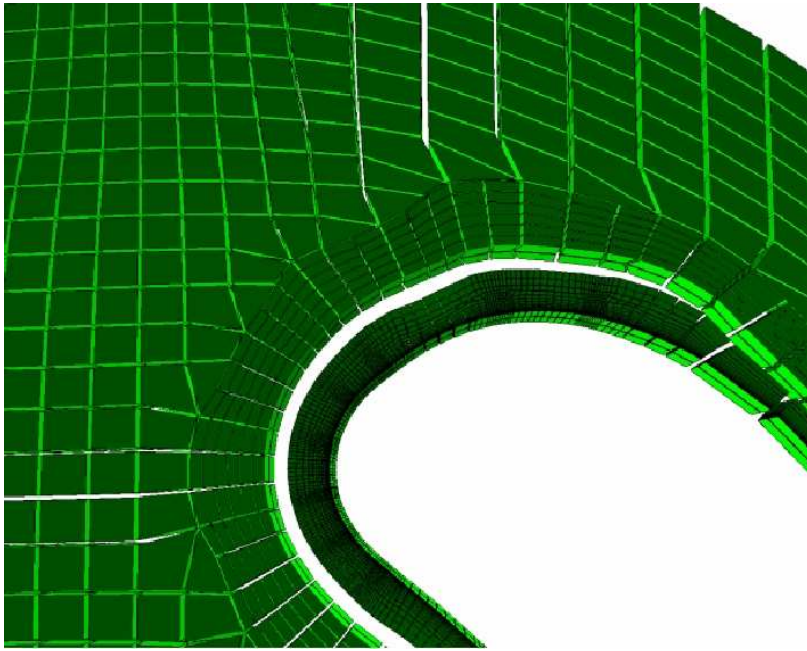


**Figure 1** A thin space between surface marching grid and particle trace grid.

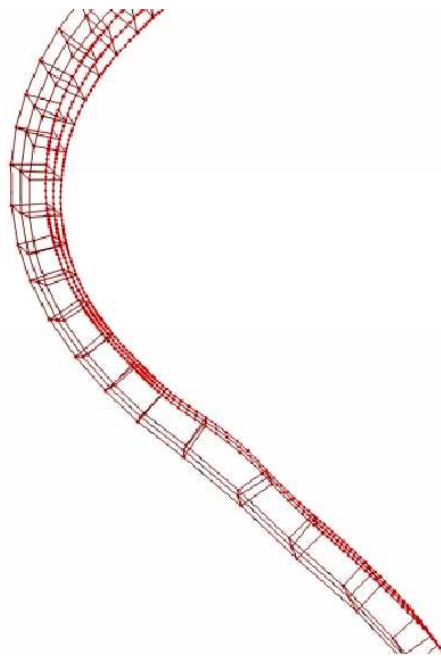


**Figure 2** Multiple fronts are formed by using shortest distance option.

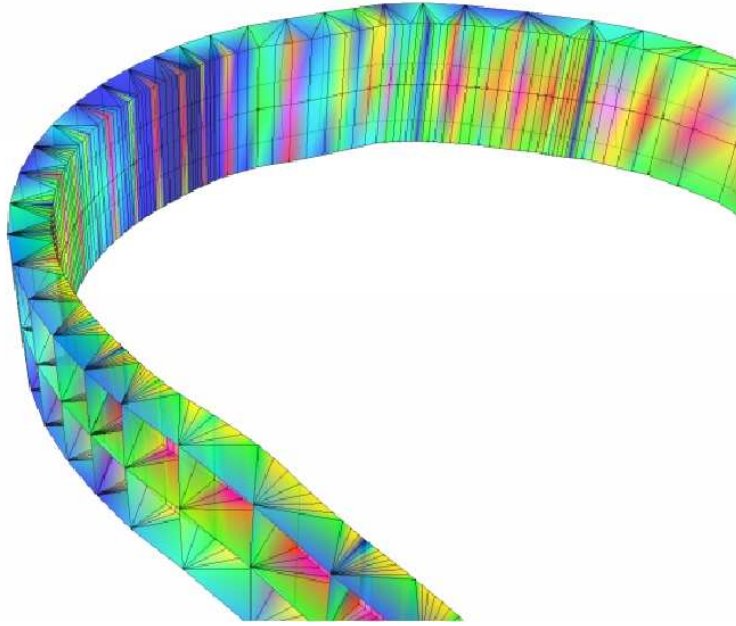


**Figure 3** Surface elements, quadrilaterals and triangles, are build for each front.— Some surface elements are removed for clarity.

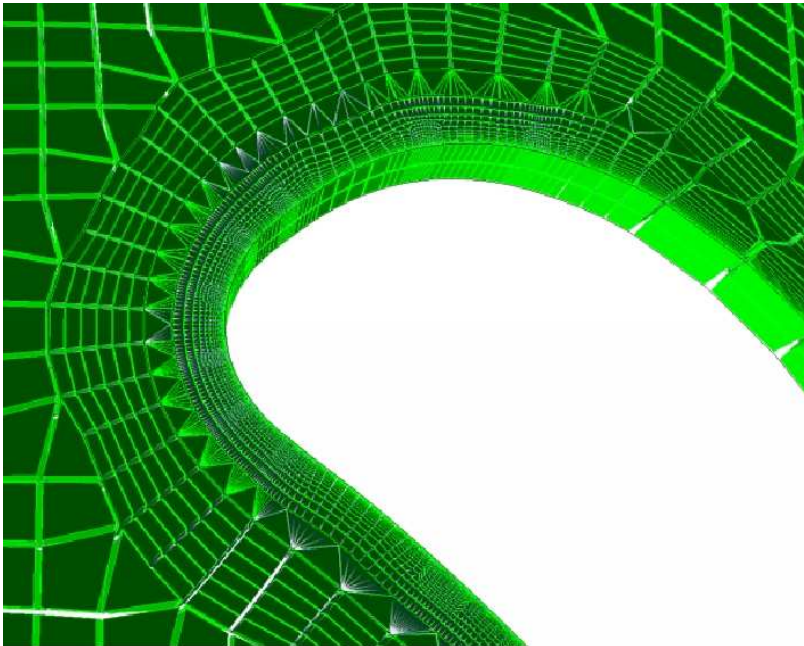


**Figure 4** Volume grid. (Note that disparity of grid resolutions is purposely created to show the robust of the method.)

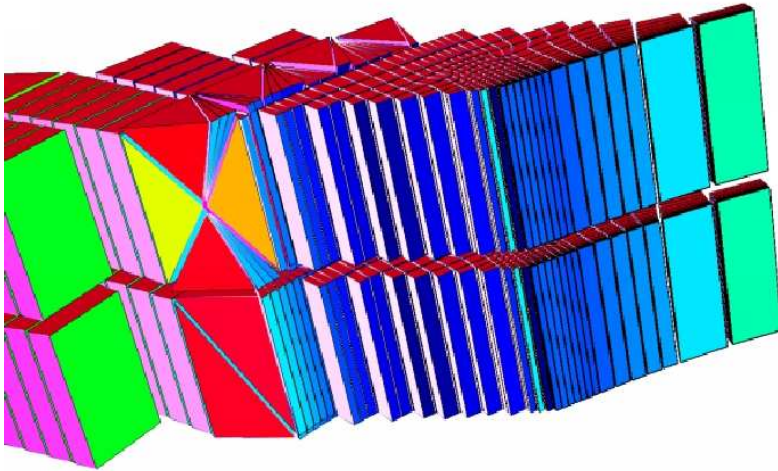


**Figure 5** A slab view of the volume grid.

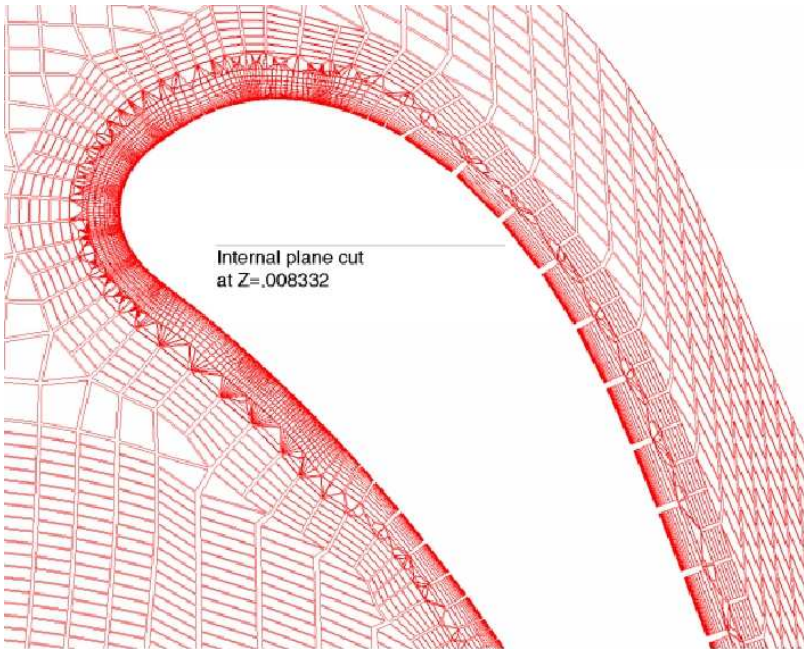


**Figure 6** A plane cut of the volume grid. The current method achieves the rapid transition of grid resolutions from the dense to the coarse in a very short distance.

## 4. CFD solution of the turbine mesh

At the mainstream inlet, the total pressure of the mainstream hot gas is set to be  $1629080 \text{ N/M}^2$ ; the total temperature is  $1644.42 \text{ K}$ ; and the specific heat at constant pressure is  $1138 \text{ J/kg K}$ . Following standard practice the value for the turbulence intensity is 4% of the computed inlet normal velocity, while the turbulence length scale at the inlet is set to be  $.05 \text{ m}$ . At the exit, the static pressure is set to be  $938350.08 \text{ N/M}^2$ ,

i.e. 57.6 % of the inlet total pressure. The surface temperature of the vane is 1151 K. The coolant mass flow is set to zero for current example. The contour plot of the static pressure for the turbine blade at a z-plane cut is shown in Figure 7. The influence due to mesh type change is minimal.

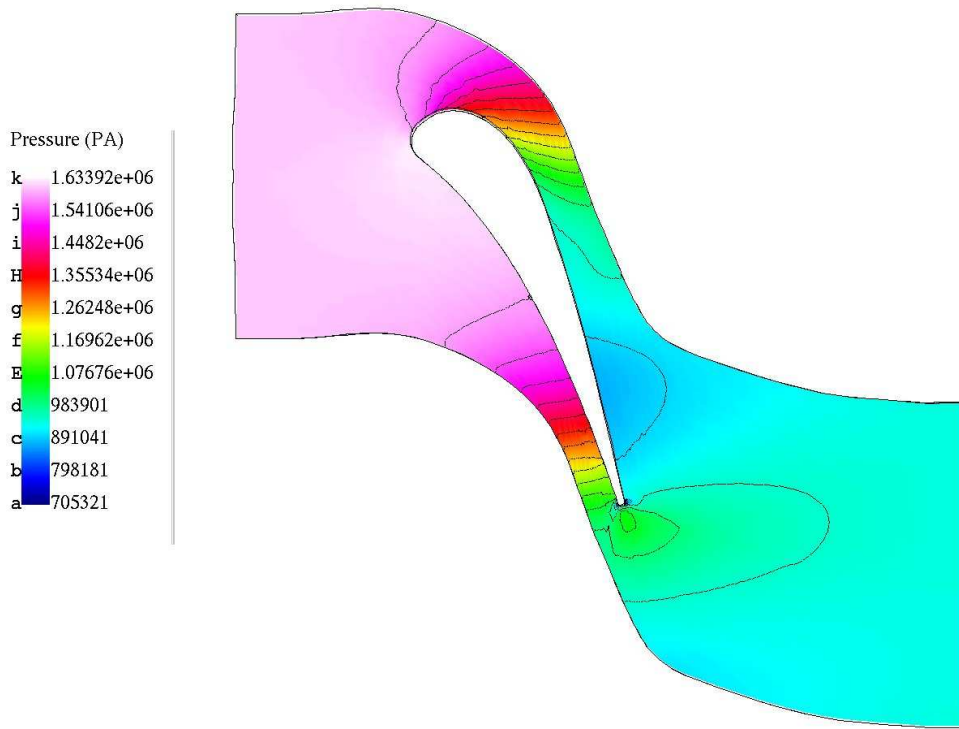


**Figure 7 Static pressure contours of a turbine blade with hybrid meshes.**

The contour plot of the static temperature for the turbine blade at a z-plane cut is shown in Figure 8. The influence due to mesh type change is also minimal.

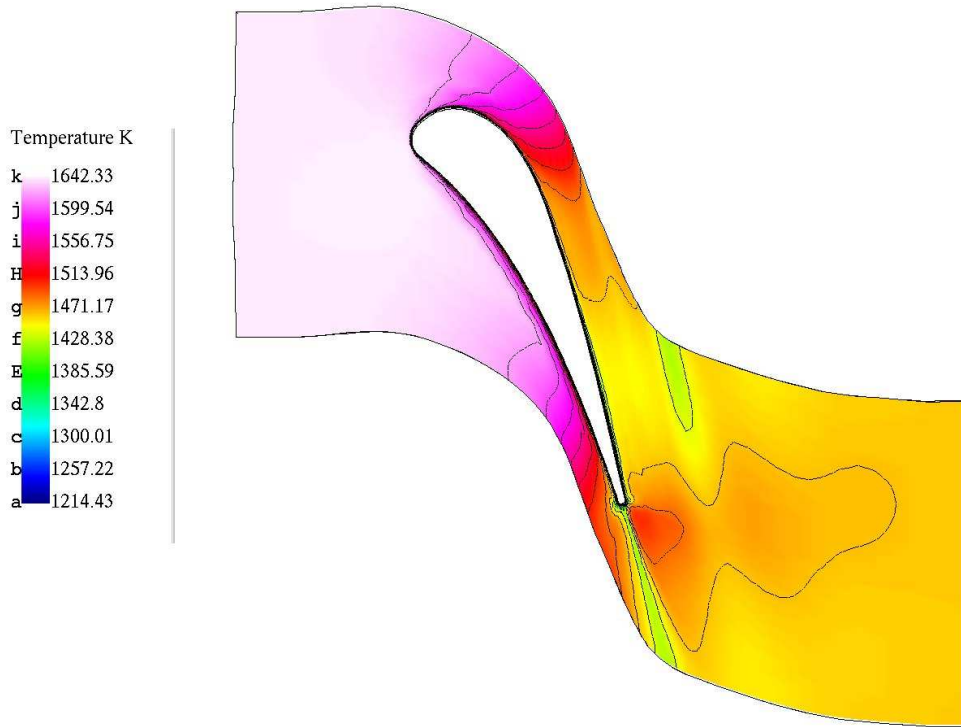


**Figure 8** Static temperature contours of a turbine blade with hybrid meshes.

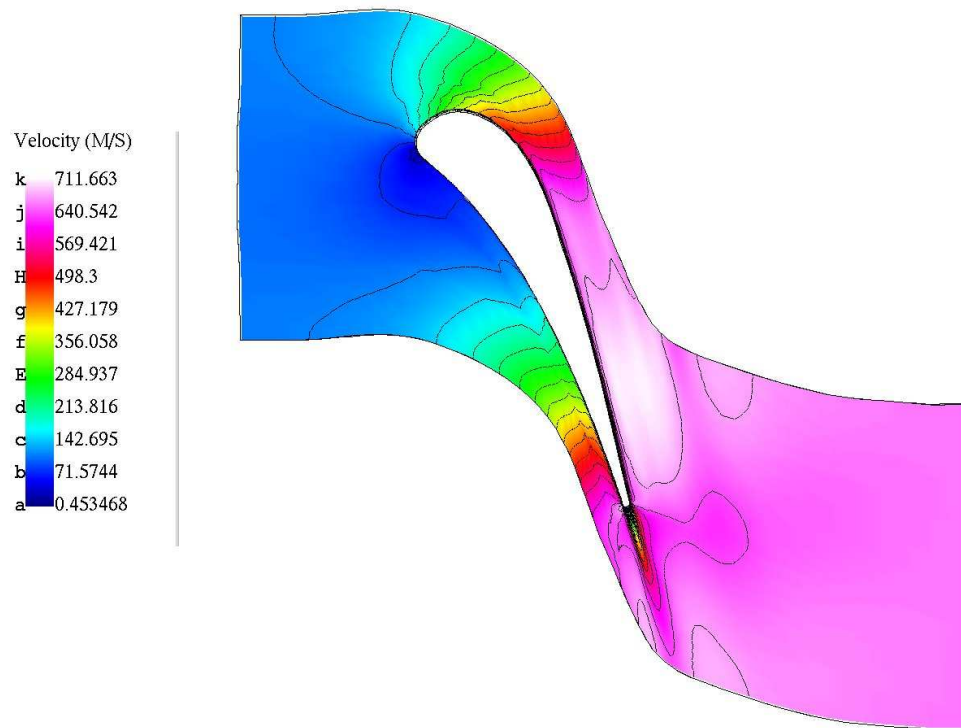


**Figure 9** A velocity contour plot.

The contour plots of the velocity and Mach number for the turbine blade at a z-plane cut are shown in Figure 9 and Figure 10, respectively. The influence due to mesh type change is noticeable on both figures.

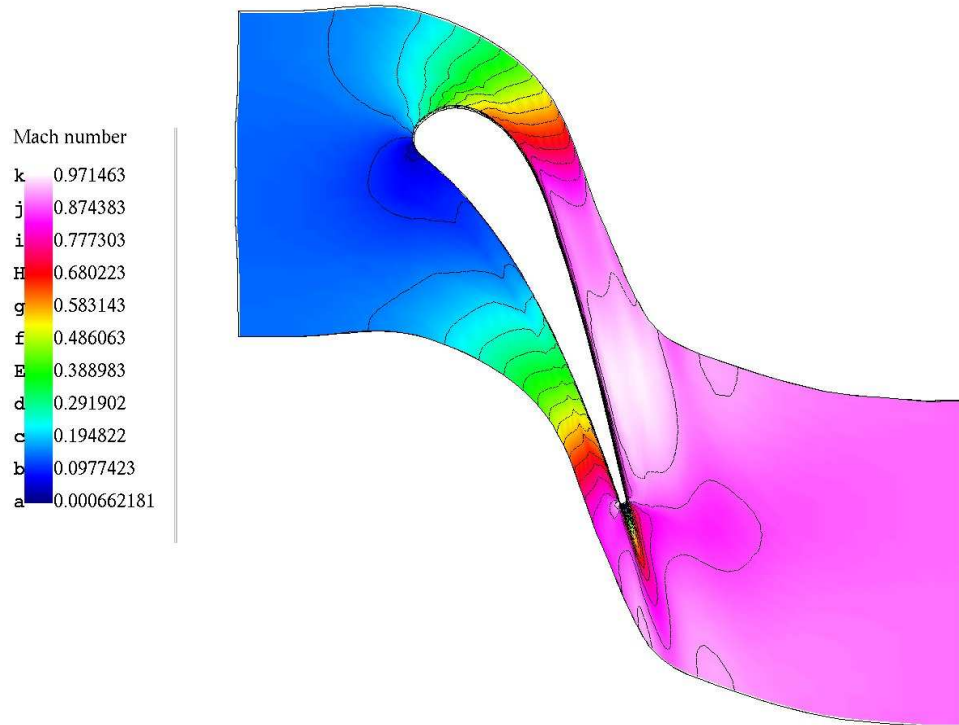


Figure 10 A plane-cut view of Mach number.

## 5. Example 2

A hexahedron-dominated mesh is generated around a simple three-dimensional cylinder and obtained an inviscid solution by NCC.

The steps to generate the current mesh are:

1. Generates algebraic marching grid from the cylinder surface.
2. Generates a box grid which is more or less influenced by cylinder marching grid.
3. Overset cylinder marching grid and box grid to builds particle trace grid guided by cylinder marching grid. Let it terminate before reaching cylinder surface.
4. A thin space is formed between two marching grids.
5. Volume grid is generated in this thin space using an advancing front method by partitioning the sub domains into pyramids, tetrahedrons and wedges. (Figure 11 and Figure 12)

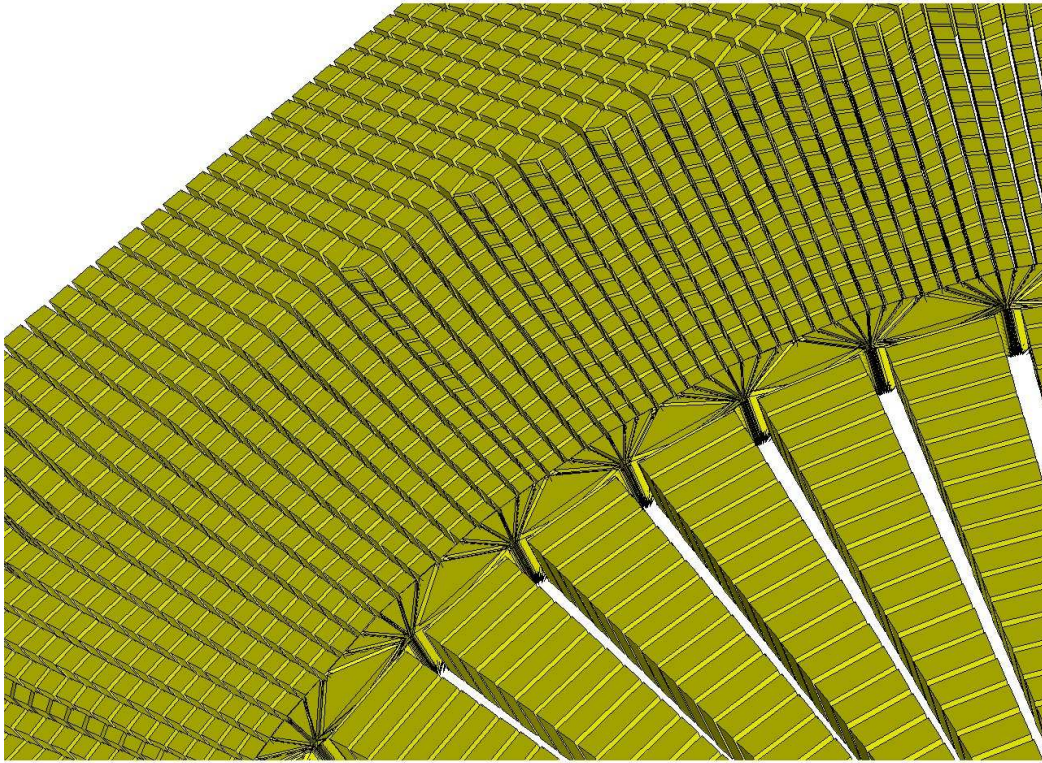


**Figure 11** A 3d mesh plot that shows hexahedrons, pyramids, wedges and tetrahedrons.

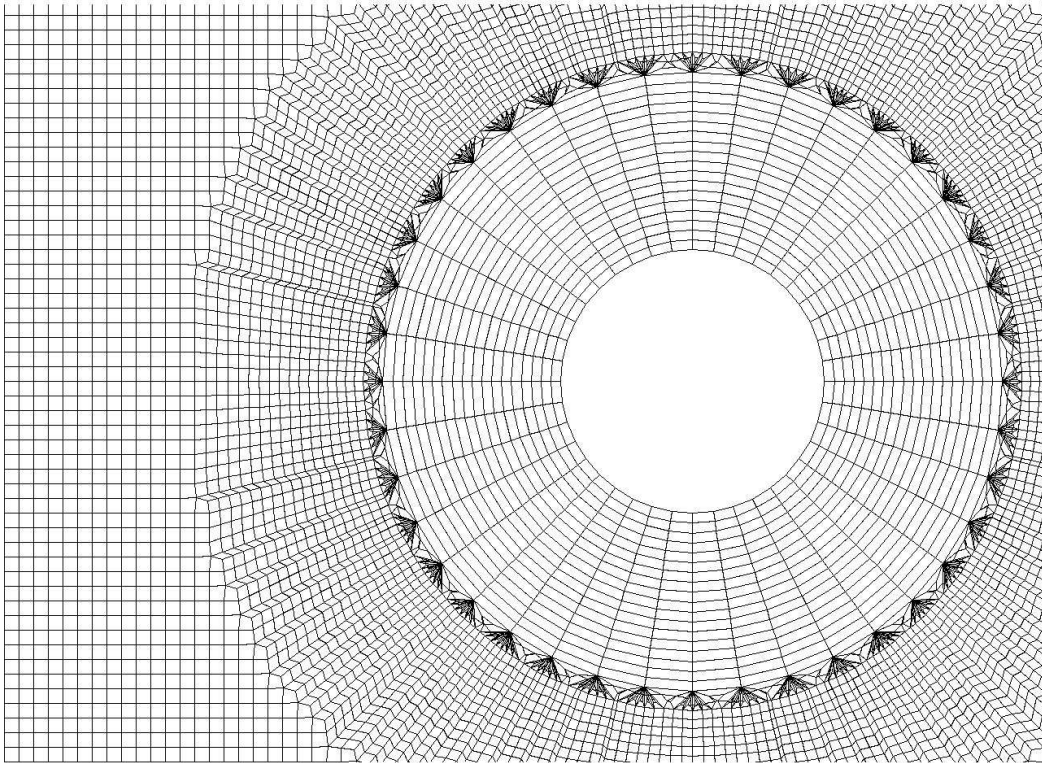


**Figure 12** Mesh transition from hexahedron to pyramid and tetrahedron and back to hexahedron.

At the left side of the box, the total pressure of the inlet gas is set to be  $1516846.6 \text{ N/M}^2$ ; the total temperature is  $1611 \text{ K}$ ; and the specific heat ratio is  $1.32$ . At the right side of the box, the static pressure of the exit is set to be  $1290265.8 \text{ N/M}^2$ , i.e.  $85 \%$  of the inlet total pressure. The contour plots of Mach number, static pressure, static temperature and velocity are shown in Figures 13-16, respectively. Due to disparity of the resolutions of the different types of grids, the results display the imperfection of the contour lines.

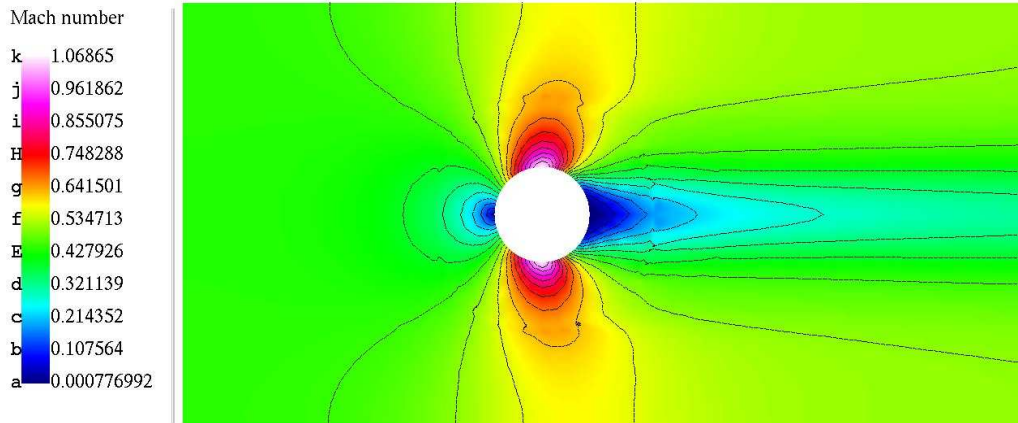


**Figure 13** Plot of Mach number contour. The contour lines that pass through the transition mesh show the influence of changing mesh types.

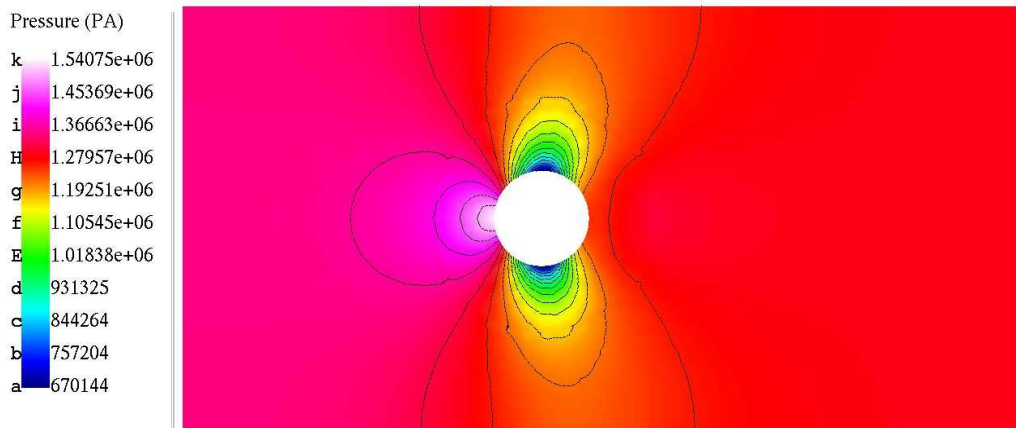


**Figure 14** Plot of pressure contour. The contour lines that pass through the transition meshes display slight imperfection.

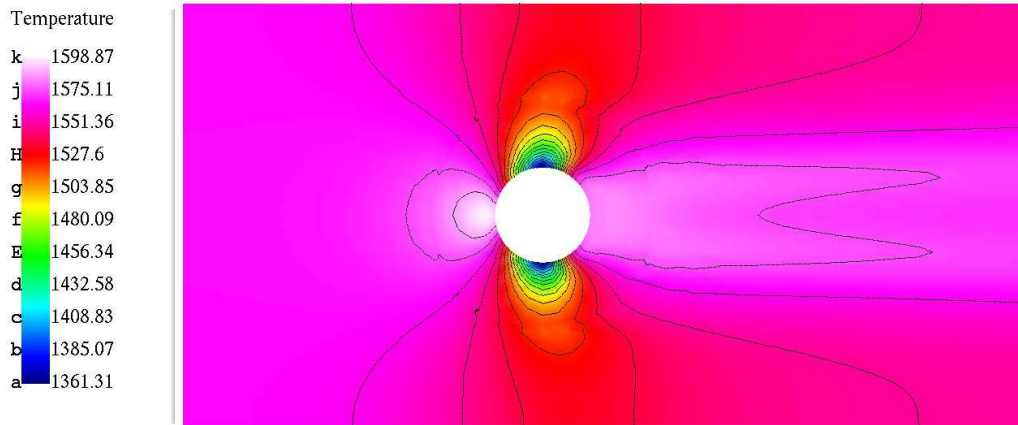


**Figure 15** Plot of temperature contour. The contour lines that pass through the transition meshes display slight imperfection. F

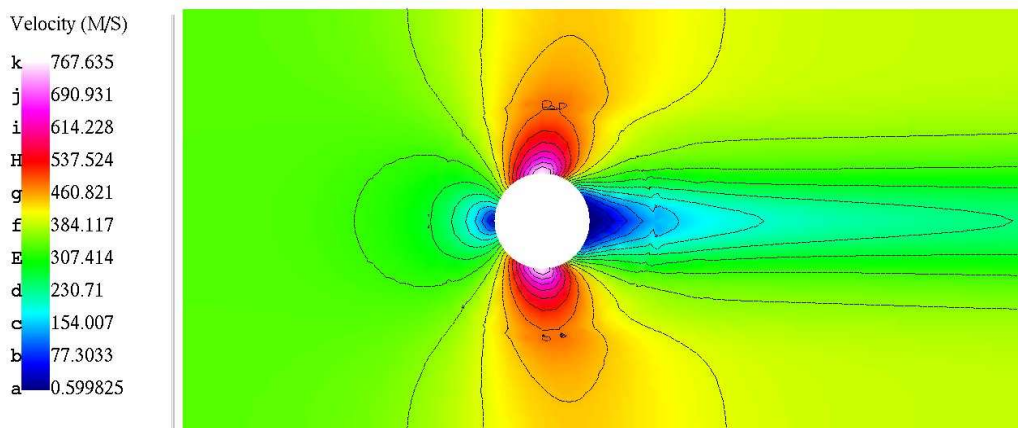


**Figure 16** Plot of velocity contour. The contour lines that pass through the transition meshes display slight imperfection.

## 5. Concluding remarks

A hexahedron mesh generation method has been modified to create hybrid meshes by merging surface marching grids and inside out grid-based meshes via an advancing front method. It results in a hexahedron-dominated conforming mesh. The surface marching grid is especially suitable for viscous flow calculation.

This mesh generation is part of a unified approach to generate unstructured (1) overset-hexahedron, (2) all-hexahedron, (3) mostly-hexahedral meshes. Three types of component grids are required to be first generated and then proceed to create any one of three meshes. These common grids are surface grid, marching grid and core grid. In the future, more realistic geometries will be used to generate the third type of meshes.

## References

- [1] T. Blacker, "Meeting the Challenge for Automated Conformal Hexahedral meshing," 9th International Meshing Roundtable, Oct., 2000.
- [2] T. C. Wey, "Unstructured Hexahedral Mesh Generation Using the Analogy of the Particle Traces — Dual Use of Overset Grid Generation Techniques," AIAA 2001-1097, 39th Aerospace Sciences Meeting and Exhibit January 8–11, 2001/Reno, NV
- [3] T. C. Wey, "The Applications Of An Unstructured Grid Based Overset Grid Scheme To Applied Aerodynamics," 8th International Meshing Roundtable, Oct., 1999.
- [4] S. Saha and B. C. Basu, "Simple Algebraic Technique for Nearly Orthogonal Grid Generation," AIAA J. Vol. 29, No.8. pp.1340.
- [5] T. C. Wey and C. P. Li, "Numerical Simulation of Shuttle Ascent Transonic Flow Using an Unstructured Grid Approach," Symposium on Computational Technology for Flight Vehicles, Nov. 5–7, 1990, Washington, D. C., also appears in Computer & Structures Vol. 39, No. 1/2, pp. 207-218, 1991.
- [6] W. M. Chan and R. J. Gomez III, "Advances in Automatic Overset Grid Generation Around Surface Discontinuities," AIAA 14<sup>th</sup> Computational Fluid Dynamics Conference June 28 – July 1, 1999.
- [7] R. Schneiders and J. Debye, "Refinement Algorithms for Unstructured Quadrilateral or Brick Element Meshes," Modeling, Mesh Generation and Adaptive Numerical Methods for Partial Differential Equations; Proceedings IMA, 1995.
- [8] R. M. Stubbs and N. S. Liu, "Preview of National Combustion Code," AIAA 97-3114, 1997.